processes

MDPI

Article

Tailings Reuse in Low-Permeability Reactive Geochemical Barriers

Roberto Rodríguez-Pacheco *, Joanna Butlanska * and Aldo Onel Oliva-González

Consejo Superior de Investigaciones Científicas (CSIC), Centro Nacional Instituto Geológico y Minero de España (CN IGME), Ríos Rosas 23, 28003 Madrid, Spain; ao.oliva@igme.es

* Correspondence: roberto.rodriguez@csic.es (R.R.-P.); j.butlanska@igme.es (J.B.); Tel.: +34-91-72872351 (R.R.-P.)

Abstract: This paper presents the physical, hydrogeological, and geochemical characterizations of two types of tailings: one from the nickel–cobalt (Ni–Co) and the other from the lead–zinc (Pb–Zn) industries. The study is restricted only to Ni and Zn ions behavior. The mineralogical composition of the studied tailings is primarily composed of oxides and hydroxides of iron, aluminum, and silica. Based on their grain size, these wastes are geotechnically classified as low plasticity silts, with permeability ranging from 10^{-8} m/s to less than 10^{-9} m/s. Batch and column flow tests, along with metal transport tests using heavy metal-contaminated wastewater, reveal that these tailings have an adsorption capacity for metals such as nickel (Ni) and zinc (Zn) ranging from 2000 to 6000 mg/kg of solid. This high adsorption capacity surpasses that of many clayey soils used for sealing municipal, industrial, mining, and metallurgical waste deposits. Additionally, these wastes can neutralize the acidity of wastewater. The results indicate that the mineralogical composition and pH of these tailings are key factors determining their adsorption characteristics and mechanisms. Due to their characteristics, these tailings could be evaluated for use as low-permeability reactive geochemical barriers (LPRGB) in the conditioning of repositories for the storage of industrial, urban, mining and metallurgical waste. This would allow large volumes of tailings to be repurposed effectively.

Keywords: tailings; geotechnical barriers; batch test; column test; metal transport

check for updates

Academic Editor: Guining Lu

Received: 28 February 2025
Revised: 27 May 2025
Accepted: 11 June 2025
Published: 13 June 2025

Citation: Rodríguez-Pacheco, R.; Butlanska, J.; Oliva-González, A.O. Tailings Reuse in Low-Permeability Reactive Geochemical Barriers. *Processes* **2025**, *13*, 1870. https://doi.org/10.3390/pr13061870

Copyright: © 2025 by the authors. Licensee MDPI, Basel, Switzerland. This article is an open access article distributed under the terms and conditions of the Creative Commons Attribution (CC BY) license (https://creativecommons.org/licenses/by/4.0/).

1. Introduction

Human activities generate substantial amounts of waste, including urban, industrial, mining, metallurgical, and radioactive wastes of varying hazard levels [1]. The safe storage of these wastes needs the construction of geotechnically and environmentally secure storage facilities. According to the current European Community legislation [2], the requirements for impermeable barriers at the bottom of waste repositories stipulate a maximum permeability limit of 10^{-9} m/s.

Despite their importance, the geochemical properties of impermeable barriers remain largely understudied. A thorough geochemical characterization of the materials used in these barriers can be conducted through laboratory analyses or in situ testing. One of the most critical aspects of geochemical behavior is the adsorption capacity of the porous matrix, typically quantified in the laboratory by determining the partition coefficient (K_d). This coefficient describes the distribution of a solute between the solid and liquid phases under equilibrium conditions across various concentration ranges. Impermeable barriers (IMBs) employed in waste disposal sites are generally composed of clayey materials with permeabilities of 10^{-9} m/s or lower. Commonly used soils include those rich in kaolinite, montmorillonite, or other types of clay. However, according to the literature reviewed [3,4], mining or metallurgical tailings have not yet been utilized for this purpose.

Considering the strictness of environmental legislation, the use of reactive geochemical barriers (RGBs) is essential in constructing tanks or reservoirs for storing waste derived from anthropogenic activities. The environmentally hazardous waste stored in these tanks can be liquid, solid, or a mixture of both. In this context, we refer to industrial, mining–metallurgical, and urban wastes, which are characterized by leaching from water contaminated with metals and, in many cases, acidic pH [5].

A LPRGBs (low-permeability-reactive geochemical barriers) consist of a porous matrix composed of one or more compacted materials placed at the base and walls of the tank where the waste is dumped. These LPRGBs hinder the passage of contaminated water due to its low permeability ($\leq 10^{-9}$ m/s). The low permeability increases the contact and reaction time between the porous medium and the pollutants.

In these barriers, the existing materials create geochemical conditions (E_h, pH) that reduce the passage of different pollutants through absorption, precipitation, reduction, or complex formation. The way these processes work depends on the problem and the type of substance (organic or inorganic) in the wastewater leaching the waste. If the objective is to remove metals derived from the oxidation of sulfides, it is necessary to create reducing conditions that favor their precipitation. For organic compounds, this can be achieved by adding electron acceptors to maintain oxidizing conditions or by creating highly reducing conditions. In the case of metals, an oxidizing medium is needed, and the pH is adjusted depending on the pollutant. Typically, alkaline conditions (pH > 7) are created, as most metals have low mobility in aqueous media under these geochemical conditions.

The establishment of a methodology for characterizing porous materials to be used in the construction of LPRGB and permeable reactive geochemical (PRGB) barriers is a subject in full development [6,7]. The characterization of these porous materials typically includes the assessment of physical properties and hydrogeological behavior. However, in many cases, the geochemical behavior (adsorption–desorption and process hysteresis) and hydromechanical behavior of the porous material under study are not considered.

It should be noted that while there is abundant information on permeable reactive geochemical barriers for treating contaminated groundwater [1,7,8], information on low-permeability reactive geochemical barriers is scarce [8]. Therefore, the aim of this work is to evaluate the physico-mechanical, hydrogeological, and geochemical (adsorption–desorption) properties of two tailings: one from Ni–Co (nickel–cobalt) and the other from Pb–Zn (lead–zinc) industries.

2. Materials

The study focuses on two types of metallurgical tailings: one from the Cuban nickel–cobalt industry (ACL stands for tailings from ammoniac carbonate leaching process) and the other from the Spanish lead–zinc industry (CART stands for tailings from floatation process from Cartagena, Spain). In Cuba, the volume of this tailings exceeds 200 million tonnes across two municipalities, with an annual increase in more than one million tonnes. In Cartagena, Spain, this waste exceeds 40 million tonnes, and approximately 140 million tonnes of seven other types of tailings are currently being studied. Table 1 presents the main characteristics of these tailings.

Table 1. The main characteristics of the wastes.

Parameter	ACL	CART	Parameter	ACL	CART
Sand < 2 mm (%)	10	36	Organic matter (%)	4.6	4.4
Silt < 0.063 mm (%)	70	52	Fe_2O_3 (%)	43.6	35.8
Clay < 0.002 mm (%)	20	12	SiO_2 (%)	4.7	30.4

Table 1. *Cont.*

Parameter	ACL	CART	Parameter	ACL	CART
Approximate effective surface (m^2/g)	82	69	MnO (%)	0.5	1.1
pH (ratio 1:2.5)	6.45	7.88	CaO (%)	0.1	5.0
Electric conductivity (mS/cm) (1:2.5)	670	956	Al_2O_3 (%)	5.1	11.1
Hydraulic conductivity	3×10^{-9}	2×10^{-9}	MgO (%)	16.2	3.8
CEC (meq/100g solid)	10.0	18.7	Amorphous Fe (%)	4.5	6.3

CEC: cation exchange capacity.

3. Methods

3.1. Experimental Conditions

The selected experimental conditions are based on current legal regulations, specifically [2,9]. Within both the European Union and Spain, the batch test is established as the standard methodology for assessing a waste material's potential to release substances into the environment. Additionally, this method evaluates the material's capacity to adsorb substances from the aqueous medium with which it comes into contact.

The continuous flow test is designed to evaluate the material's total adsorption capacity, as it most closely simulates the conditions found in a real landfill. The procedure begins with the injection of a solution containing the solute until the material reaches saturation. This is followed by the injection of distilled water at pH = 6.5.

Distilled water is used because it represents the most unfavorable conditions that material might encounter under natural conditions. The closest real-world equivalent would be direct contact with rainwater, which typically has a pH of 6 or higher. However, this scenario does not apply to the barrier layer, as it is located at the bottom of the landfill and is not directly exposed to rainfall.

The metal concentrations selected for this study are significantly higher than those typically found in leachates from urban and industrial landfills, as well as in acid mine drainage. For instance, nickel concentrations in urban landfill leachates are around 0.08 mg/L and zinc concentrations are approximately 0.01 mg/L. In industrial landfill leachates, concentrations reach up to 0.1 mg/L, which is similar to those observed in acid mine water [10,11].

The sealing requirements for landfills, as established by the European Union, are summarized in Table 2. Both waste materials under study comply with the specified permeability criteria.

Table 2. Impermeable barrier requirements according to the type of waste to be stored in the landfill [2].

Class of Waste	Type of Waste Deposit	Saturated Permeability (m/s)	Thickness of the Impermeable Layer (m)
CIII	hazardous waste	1.0×10^{-9}	5.0
CII	non-hazardous waste	1.0×10^{-9}	1.0
CI	inert (non-reactive waste	1.0×10^{-7}	1.0

3.2. Batch Tests with Adsorption and Desorption Processes

The adsorption and desorption isotherms were obtained in the laboratory at a controlled temperature of 22 ± 2 °C using batch tests. The metal solutions were prepared in 0.01 mM of KNO_3 as the supporting electrolyte at pH = 5.5. This solution stabilizes the ionic strength, maintains the charge of the solid mineral or non-mineral particles, and ensures a consistent level of aggregation in the porous medium. In batch tests, divalent metal solutions such as $CaCl_2$ and $MgCl_2$ are commonly used as electrolytes. The tailings

from the Cuban industry are characterized by a high magnesium content (12%) and a low calcium content (≤0.1%). In contrast, CART wastes have a higher calcium content (4.5%) and a much lower magnesium content (3.8%).

In electrolytic solutions containing divalent charged elements such as Ca and Mg, it has been demonstrated that they enhance metal adsorption [9]. Based on this criterion, along with existing studies on Ni adsorption in soil using KNO_3 as an electrolytic solution—which have shown promising results—and considering the characteristics of our materials, we chose to use the same solution as in the works of [3,12].

The adsorption—desorption tests were carried out with a 1:10 ratio using the following steps:

1. Samples of 2 g of solid residue were placed in a plastic tube (volume of 40 cm^3) and brought into contact with 20 mL of a 1 mM KNO_3 solution at pH = 5.5. The samples were then agitated for 24 h to stabilize the ionic strength of the aqueous solution and the ionic charge of the particles.
2. After 24 h, they were centrifuged for 10 min at 900 rpm. separating the solid phase from the liquid phase.
3. At the end of step 2, the solid samples were washed in two stages: first, with Milli-Q water at pH = 5.5, and then with a dilute 0.01 mM KNO_3 solution at pH = 5.5. A liquid volume of 20 mL was used for both washes. In the first stage, the samples were shaken for one hour, centrifuged at 900 rpm, and the solid phase was separated from the liquid phase. In the second stage, the samples were shaken for 24 h, centrifuged for 10 min at 900 rpm, and the solid phase was separated from the liquid phase.
4. After step 3, 20 mL of solution with different concentrations of metal in each container was added to the solids.
5. The solid samples in contact with the metal solutions were placed on a rotary shaker at 10 rpm and allowed to equilibrate for the following time intervals: 5, 10, 30, 60, 120, 240, 480, and 1440 min. This process was conducted to obtain the adsorption isotherm and adsorption kinetics.
6. At the end of each time interval, the solution was centrifuged for 10 min at 900 rpm and then filtered through a 0.45-micron Millipore filter to separate the solid phase from the liquid phase.
7. The pH of the filtered aqueous solution was measured, and the solute concentration was determined by ICP-AES.
8. After step 6, the solid phase used in the adsorption process (at the points where the metal was not completely adsorbed from the solution) was contacted with a dilute aqueous solution of 0.01 mM KNO_3 without metal. The samples were then placed in a shaker at 10 rpm and allowed to equilibrate for the following time intervals: 5, 10, 30, 60, 120, 240, 480, and 1140 min, to obtain the desorption isotherm and desorption kinetics.
9. Steps 6 and 7 were repeated.

Desorption was carried out using the same methodology as the adsorption process tests, starting from step 5. The only difference was that in the desorption process, the electrolyte solution did not contain any metals or reactive agents.

In all adsorption tests, the initial pH of the solution (step 4 of the methodology) determined the concentration of the metal used in the Ni(II) and Zn(II) tests. The difference between the initial and final solution concentrations is attributed to the adsorption capacity of the residues.

Different concentrations of Ni(II) and Zn(II) were used to determine the adsorption curve. Metal solutions were prepared using nitrate salts. For nickel (Ni), the solutions were made with $Ni(NO_3)_2$ at concentrations of 0.1, 0.4, 0.75, 1.0, and 2.0 mM. Similarly, for zinc

(Zn), the solutions were prepared using $Zn(NO_3)_2$ at the same concentration levels: 0.1, 0.4, 0.75, 1.0, and 2.0 mM.

The mass of metal adsorbed per unit mass of solid (S_a) in each of the batch tests was determined by the difference between the concentration in the initial solution (C_o) and the concentration in the final solution (C_w):

$$S_a = \frac{(C_o - C_w)\cdot V}{M}, \quad (1)$$

where M is a total mass of residue and V is a volume of electrolyte solution.

The mass of desorbed solute (S_d) was determined by the difference between the initial concentration of the aqueous solution without solute (C_{wi}) and the concentration in the final aqueous solution (C_{wf}) after its interaction with the soil mass used in the adsorption process:

$$S_d = \frac{\left(C_{wf} - C_{wi}\right)\cdot V}{M}. \quad (2)$$

Determining the adsorption isotherm is essential for estimating the various parameters that control the flow and transport of contaminants in porous media. In this study, the adsorption isotherm can be described using the Freundlich Equation (3) and Langmuir Equation (4), assuming that equilibrium has been reached in the residue–liquid solution:

$$\begin{gathered} S = K_d\cdot(C_w)^n \text{ para n} \neq 0 \\ \log_{10} S = n\cdot\log_{10} C_w + \log_{10} K_d \end{gathered} \quad (3)$$

$$S = \frac{K_L\cdot C_w}{1 + K_L\cdot C_w}, \quad (4)$$

where K_d, K_L and n are a constant whose values can be obtained from the adsorption isotherm by a least-squares fit.

In the batch tests involving pH-dependent adsorption processes, the determination of the adsorption process was conducted as a function of pH. The results indicated that the pH shifted from the initial soil value of 6.45 for the ACL tailings and 7.88 for the CART tailings to 2 upon the addition of nitric acid and to 10 upon the addition of sodium hydroxide.

3.3. Transport and Flow Tests of Solutes

Transport and flow tests were conducted using a tracer (pentafluorobenzoato, PFB) and the metals Zn(II) and Ni(II). The objective of the tracer test was to physically characterize the porous medium. Both the tracer test and the metal flow and transport test utilized the same electrolyte solution ($Ni(KNO_3)_2$) as in the batch tests. The metal concentration used in the waste column inlet solution for Zn(II) and Ni(II) is significantly higher (416 mg/L) than the concentrations typically found in contaminated wastewater.

The PFB test is conducted independently of Ni(II) and Zn(II) to avoid interference. PFB acts as a conservative tracer, used to characterize the properties of the porous medium prior to conducting flow and transport experiments with reactive metals. These reactive metals can alter the system's behavior, so establishing baseline conditions with a non-reactive tracer is essential for accurate interpretation.

A Spectra System HPLC (high-performance liquid chromatography) apparatus was used for the flow tests (https://www.agilent.com/ (accessed on 15 January 2025)). This system features two double-piston pumps (P2000) that maintain a stable flow rate ranging from 0.01 to 9 mL per minute. An in-line diode array detector (UV-600LP, Thermo Electron Corporation, Madrid, Spain) continuously detects solutes within a wavelength range of 190 to 800 nanometers. The entire system is managed through a computer using the

CHROMQUEST software version 2.1, which also generates files for export to MS-DOS for modeling purposes.

The column (Figure 1) was filled with solid tailings dried at 46 ± 2 °C to prevent the loss of organic matter. The packing of the column was performed in multiple compaction steps using vibrations to achieve a uniform density and to prevent cavity formation, which could lead to preferential flow. The column was then saturated with a 0.1 mM KNO_3 electrolytic solution, identical to the one used for the adsorption isotherms. Saturation lasted 24 h to remove air bubbles. Afterward, the electrolyte solution was passed through the column at a rate of 1.2 cm/h until steady flow conditions were achieved. This was confirmed by ensuring that the flow rate (Q), pH, and electrical conductivity of the inlet and outlet solutions were identical. Table 3 summarizes the main characteristics of the columns used in the flow and transport tests for reagent solutes and tracers.

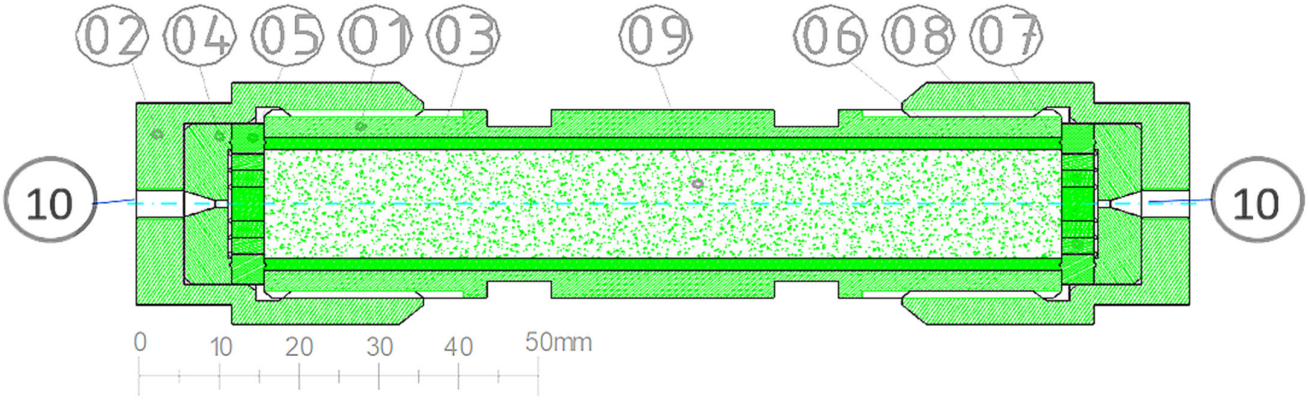


Figure 1. Diagram of the column used in the laboratory: 01—steel wall; 02—locking nut; 03—plastic wall; 04—plastic toric for fitting the connectors; 05—fitting toric between the plastic tube and the outer toric; 06, 07, and 08 are the concentric rings that act as a filter and evenly distribute the water; 09—sample of the solid; 10—the blind volume (V_m) that corresponds to the volume of the inlet and outlet pipes of the waste column.

Table 3. Main characteristics of the tailings' columns used in the flow and transport tests.

Parameter	Units	ACL	CART	Parameter	Units	ACL	CART
Length (L)	cm	10.00	10.00	Apparent density (ρ_h)	g/cm^3	2.11	2.12
Diameter (Φ)	cm	1.60	1.60	Dry density (ρ_h)	g/cm^3	1.44	1.53
Total volume (V)	cm^3	20.11	20.11	Pore Volume (V_p)	cm^3	12.22	12.9
Blind volume, (V_m)	cm^3	0.121	0.112	Porosity (n)	cm^3/cm^3	0.61	0.64
Tailings mass (M)	g	30.66	30.70	Flow velocity (v)	cm/h	1.2	1.2
Volumetric water content (θ)	cm^3/cm^3	0.61	0.64	Particle density (ρ_s)	g/cm^3	3.97	3.85

3.4. Mesurement of Metal Concentration and pH

The concentrations of Ni and Zn in the solutions before and after equilibrium were determined by AA6300 Atomic absorption spectrometer (Shimadzu, Kyoto, Japan). The pH of the solution was measured with a Hanna pH meter using a combined glass electrode.

3.5. Mesurement of Mineral Composition Using X-Ray Diffraction

A tailings sample for X-ray diffraction was air-dried and gently grounded by hand with a mortar and pestle. The mineral phases were identified by powder XRD using a Bruker D8 Advance instrument in θ–θ mode (Bruker Corporation, Billerica, MA, USA), with CuKα radiation, 40 kV, 30 mA, and a 1-dimensional detector with a window of 2°.

A tailings sample size of approximately 1–2 g was used to perform the analysis. The samples were step-scanned from 5 to 70° in 2θ, with 0.05° stepping intervals, 1 s

per step, and a rotation speed of 30 rpm. The powder samples were mounted in back-loading plastic holders. The diffraction patterns were evaluated with DIFFRAC.EVA version 3.0 (a commercial package from Bruker AXS, Karlsruhe, Germany, 2012) and the powder diffraction files database PDF4+ (https://www.icdd.com/pdfsearch/ (accessed on 15 January 2025).

4. Results

4.1. Mineralogical Composotion of Mine Tailings

Figure 2 shows the diffractogram of the two types of residues studied. The predominance of iron oxides and hydroxides hematite can be seen in the case of the ACL residue and goethite in the CART residue.

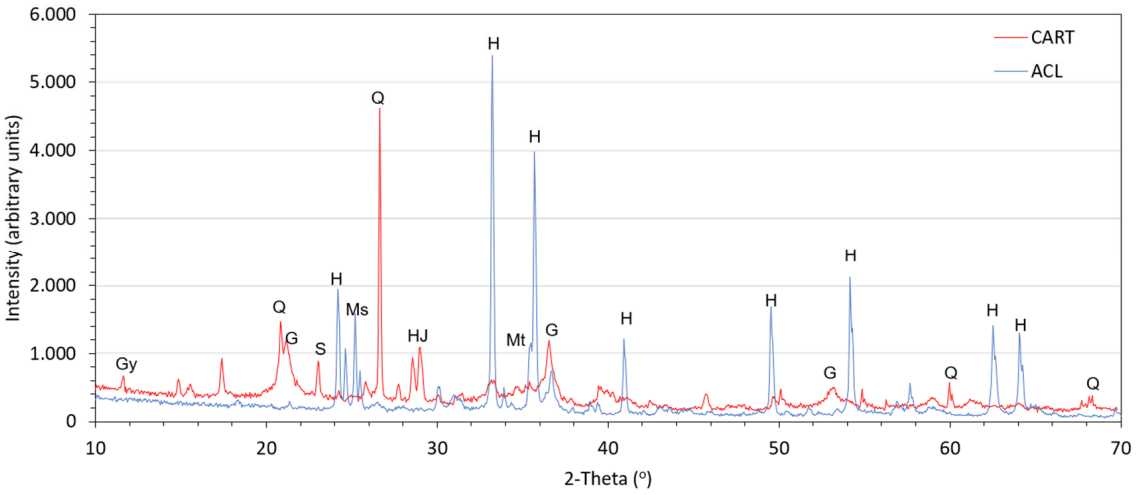


Figure 2. General information content of a powder diffraction pattern in mine's tailings. Q: quartz, G: goethite, Mt: magnetite, H: hematite, Gy: gypsum, J: jarosite: S: magnesium sulfate.

4.2. Batch Tests

From the time-dependent adsorption experiments, it can be observed that the adsorption equilibrium between the solid and the liquid is practically reached after 8 h for Zn in both tailings (Figure 3). In the ACL, the equilibrium time is even shorter. This behavior is similar for the other metals studied (Ni, Cr, Mn). The rapid attainment of adsorption equilibrium suggests that the predominant adsorption mechanism is electrostatic attraction forces, controlled by the charge of the solid particles (zeta potential).

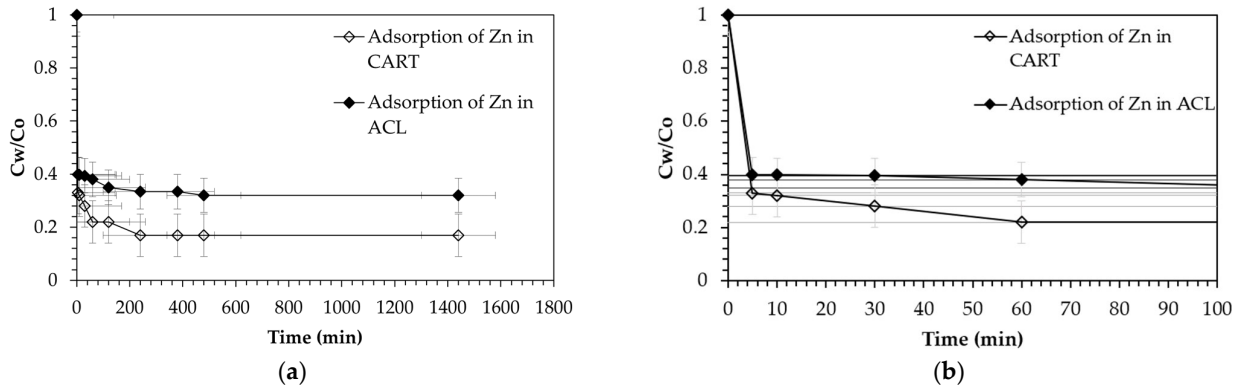


Figure 3. (**a**) Adsorption versus time and (**b**) details at the initial time. C_o: concentration in the initial solution (C_o = 416 mg/L), C_w: concentration in the final solution.

Figure 3 shows that more than 60% of the mass is adsorbed in less than 5 min, with 100% adsorption reached by approximately 8 h.

The tailings exhibit non-linear adsorption isotherms for both metals, while desorption isotherms are linear, indicating limited irreversibility and significant hysteresis. Figure 4 illustrates the hysteresis observed in the Ni(II) and Zn(II) adsorption process, a trend consistent across two metals studied. The hysteresis is particularly pronounced in the ACL residue, where the effective mass of solute retained under these test conditions exceeds 1800 mg/kg. This highlights the high capacity of the ACL to retain the mass of Ni(II) initially adsorbed. Table 4 presents the parameters of the adsorption and desorption isotherms for these metals. The data show a good correlation coefficient, fitting well with the Freundlich equation (Equation (3)). The K_d values for the CART are notably higher for Zn(II) and Ni(II), whereas the values for the ACL are approximately 50% lower. These high partition coefficient (K_d) values indicate strong binding of these elements to the surface of the solid particles in the waste matrix.

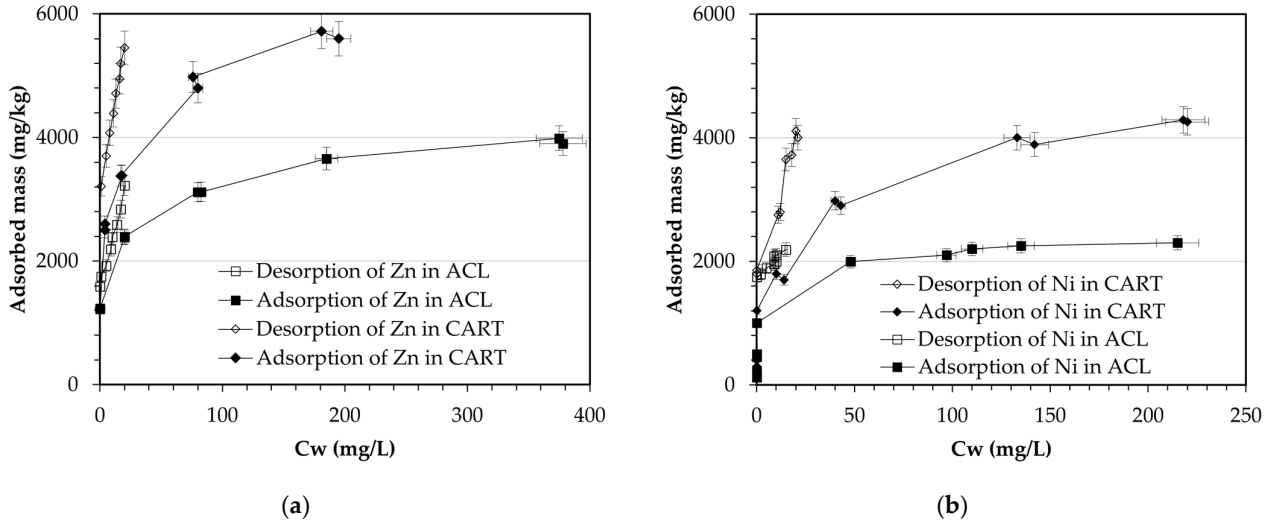


Figure 4. Adsorption and desorption isotherms of (**a**) Ni(II) y (**b**) Zn (II) for ACL tailings (Cuba) and CART tailings (Spain).

Table 4. K_d, n values and uncertainties calculated for the two residues from the fit to the Freundlich equation [13] in the adsorption and desorption isotherms.

Tailings	Metal	N	K_d	n	r^2	log(σa)	σn	N	K_d	r^2	σa	σb
			Adsorption						Desorption			
CART	Zn(II)	14	2347	0.15	0.97	0.02	0.01	14	119.06	0.99	2.87	36.92
	Ni(II)	13	1194	0.24	0.91	0.03	0.04	14	109.5	0.96	8.76	126.03
ACL	Zn(II)	14	1962	0.11	0.97	0.01	0.006	14	76.24	0.98	4.01	46.9
	Ni(II)	9	1351	0.101	0.91	0.03	0.02	9	30.27	0.91	3.83	33.6

log(σa), σn and σa, σb are uncertainties of linear fitting y = ax + b or log(y) = n × log(x) + log(a). r^2 = correlation coefficient, N = number of samples.

4.3. Adsorption of Metals as a Function of pH

Adsorption in porous media is typically governed by redox conditions, particularly pH and E_h. Among these parameters, the pH of the medium and the mineralogy of the porous matrix play a dominant role. Figure 5 shows that the highest adsorption values occur at pH levels above 6, reaching a maximum in alkaline conditions (pH > 7). For Zn(II), the adsorbed mass is 40% higher than that of Ni(II) at pH > 7.

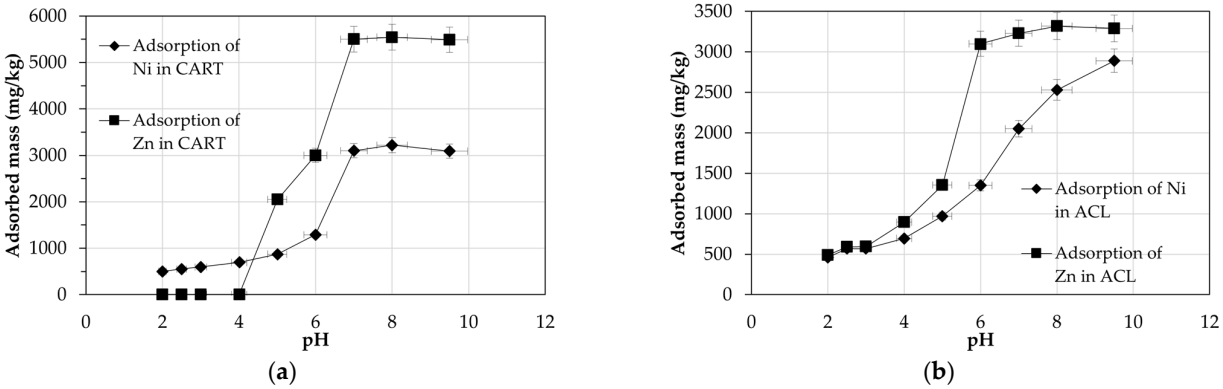


Figure 5. Adsorption of Zn(II) y Ni(II) as a function of pH: (**a**) CART tailings and (**b**) ACL tailings. (The initial used concentration, C_o = 416 mg/L).

4.4. Column Solute Transport and Flow Test

For each soil column in which the metal test is performed, the tracer test with pentafluorobenzene (PFB) is first carried out at the same flow rate to obtain the PFB breakthrough curve (Figure 6a). The analysis of this curve is usually performed using the method defined by [14]. This statistical analysis allows us to deduce the conditions under which the test is performed and to check for non-equilibrium or preferential flow conditions. The results in Figure 6a show that the PFB curve is almost symmetrical and has a uniform plateau and a very small tail. This confirms that the column is physically stable and that, apparently, there are no non-equilibrium processes or preferential flow in the medium, since the test reaches saturation for a pores volume.

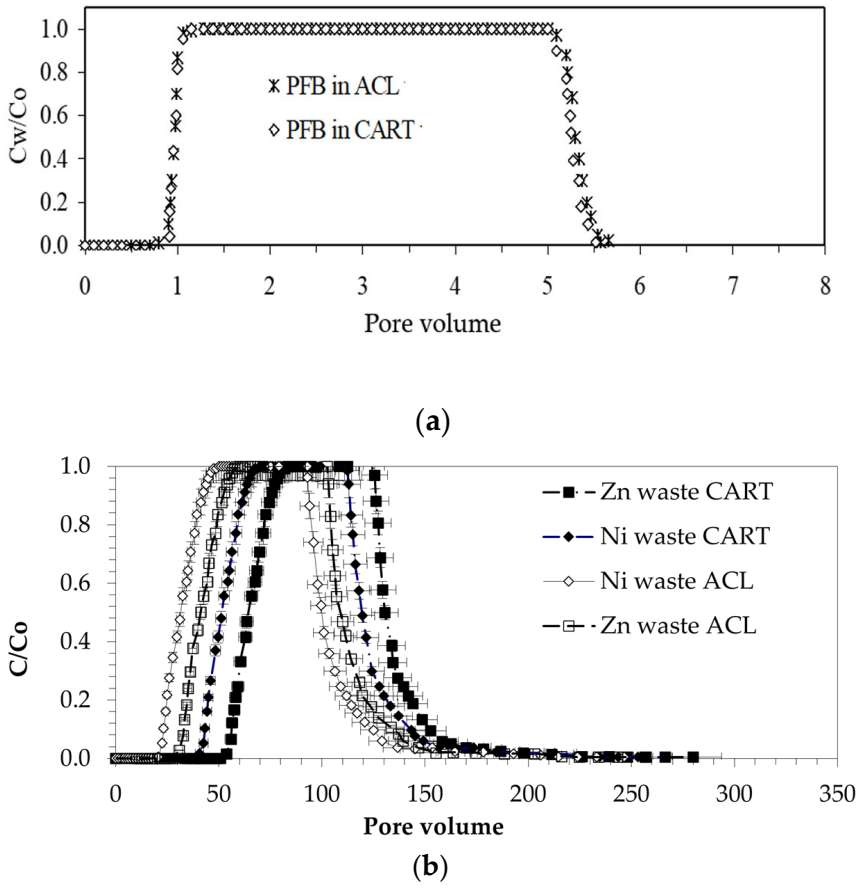


Figure 6. Breakthrough curve in the test of (**a**) flow and (**b**) transport of Zn(II) and Ni(II) in the two residues. (Initial concentration, C_o = 416 mg/L and flow velocity, $v = 2.8 \times 10^{-6}$ m/s).

Flow tests with Zn(II) and Ni(II) were conducted under conditions specified in Table 3. The Ni(II) arrival curve through the two residues shows the effects of non-ideal non-equilibrium flow conditions, presenting a large tail (Figure 6b). To reach a $C_w/C_o \approx 1$ concentration—indicating saturation of the adsorption zones—more than 20 pores volumes are required for both metals in both residues. These findings suggest a prolonged transit time for the contaminants through the porous medium.

The low metal concentration in the effluent, even when the solid's adsorption capacity is saturated, is noteworthy because these concentrations are environmentally assimilable. The maximum adsorbed solute mass (S_{max}) in the CART tailings is significantly higher than in the ACL tailings, although both retain a considerable amount of mass. This difference is due to the pH variation between the two residues and the higher content of amorphous Fe in the CART.

In neither residue does the concentration reach zero at the end of the flow and transport test. However, the concentrations are below the limits allowed for wastewater discharge, which is 20 mg/L for Zn [15]. For toxic metals, the limit is set at 3 mg/L, while no specific limit is established for Ni, although the threshold for drinking water is 0.05 mg/L (Figure 5, Table 5).

Table 5. Main results of the waste flow and transport tests.

Tailings		pH_{Co}	pH_a	pH_d	PV_i	PV_d	v (m/s)	C_o (mg/l)	C_{wf} (mg/l)	S_{in} (mg)	S_{rec} (%)	S_{ret} (%)
CART.	Zn(II)	5.67	7.30	7.32	124	156	2.8×10^{-6}	416	0.01	665.43	80.5	19.5
	Ni(II)	5.70	7.28	7.26	111	169	2.8×10^{-6}	416	0.02	595.67	90.3	9.7
ACL	Zn(II)	5.67	6.84	6.90	102	178	2.8×10^{-6}	416	0.021	518.52	86	14
	Ni(II)	5.70	6.81	6.92	93	187	2.8×10^{-6}	416	0.03	472.77	96	4

pH_{Co}. at initial concentration; pH_a in the effluent after adsorption; pH_d of the effluent after desorption. PV_i: volume of solution pores injected (adsorption); PV_d: volume of pores injected without metal (desorption); v: flow rate; C_o: initial concentration; C_f: final concentration; S_{in}: mass injected; S_{ret}: percentage of mass retained in the porous matrix; S_{rec}: mass recovered at the end of the experiment.

An analysis of the results presented in Table 5 reveals that the mass retention efficiency in the flow test is 61% for Zn and 80.6% for Ni in the case of the CART tailings. For the ACL tailings, the adsorption efficiency is even higher, reaching 72% for Zn and 92% for Ni.

These tailings also exhibit a remarkable ability to neutralize acidity. Although the contaminated water entering the column is consistently acidic, the effluent exits with a pH level similar to that of the residue in the field.

4.5. Main Chemical Reactions

The adsorption of nickel and zinc onto hematite and goethite can be described using equilibrium models such as the Langmuir and Freundlich isotherms, which enable the calculation of the equilibrium constants for the process. This adsorption is a complex phenomenon involving surface interactions and the formation of surface complexes on iron oxides and hydroxides.

Some of the most relevant chemical reactions involved in the adsorption process include

1. Surface interaction of nickel or zinc with hydroxyl groups of hematite or goethite:

$$FeOH + Ni^{2+} \rightleftharpoons FeONi^{+} + H^{+}$$

$$FeOH + Zn^{2+} \rightleftharpoons FeOZn^{+} + H^{+},$$

where the equilibrium constant K is defined as

$$K = [FeOZn^{+}][H^{+}]/[FeOH][Zn^{2+}]$$

$$K = [FeONi^+][H^+]/[FeOH][Ni^{2+}].$$

2. Precipitation of nickel hydroxide and zinc on the surface of hematite or goethite:

$$Ni^{2+} + 2OH^- \rightleftharpoons Ni(OH)_2(s)$$

$$Zn^{2+} + 2OH^- \rightleftharpoons Zn(OH)_2(s).$$

With a solubility constant K_{sp} that depends on the pH and the concentration of ions in solution.

3. Adsorption through surface complex formation:

$$Fe_2O_3 + Ni^{2+} + H_2O \rightleftharpoons Fe_2O_3{}^-Ni^{2+} + 2H^+$$

$$Fe_2O_3 + Zn^{2+} + H_2O \rightleftharpoons Fe_2O_3{}^-Zn^{2+} + 2H^+$$

This process can be described by a stability constant K_{ads}. For the specific values of the equilibrium constants, one can refer to experimental studies such as [16,17], which analyze the adsorption behavior of heavy metals on various materials. These studies provide detailed insights into the thermodynamic parameters and surface complexation mechanisms involved in the interaction between metal ions and mineral surfaces.

5. Discussion

Based on the adsorption results, it can be concluded that adsorption occurs relatively quickly (Figure 3). The rapid rate of adsorption suggests that most of the adsorbed mass is due to purely physical mechanisms, with electrostatic forces (such as particle charge or zeta potential, Table 6) playing a fundamental role in the adsorption process. The contribution of possible chemisorption processes is likely minimal, given the time intervals used in the experiments. This observation was confirmed by X-ray diffraction (XRD) analysis, which showed no presence of clay minerals in both residues. Consequently, ion exchange processes play a lesser role, as the residues have low cation exchange capacities (CEC), with values of 10 and 18 meq/100 g of solid residue for the ACL and CART tailings, respectively (Table 2).

Table 6. The main minerals present in the tailings and the pH value at which the surface charge of the particles is zero.

Mineral	Formula	[18] pH in KNO_3 Solution	pH [19] (p. 163)	pH [17] (p. 154)	pH [16] (p. 134)	Specific Surface, *Se* (m^2/g)
Hematite	α-Fe_2O_3	8.5		8.5	6.7	85 [20]; 22 [18]
Goethite	α-FeOOH		3.2	7.3		75 [20], 28–91 [18]
Maghemite		6.8	6.7			
Magnetite		6.2 [20]				85 [20]
Amorphous aluminum	$Al(OH)_3$		8.3	5.0		
	AlOOH	9.2				
Amorphous iron	$Fe(OH)_3$		8.5	8.5	8.5	
Ferrihydrite	Fe_5OH_8 $4H_2O$	8.1	8.1			600 [21]
Gibbsite	α-$Al(OH)_3$	7.1	4.8		5	18–47 [18]
Quartz	SiO_2	2		2.9	2.0	
Calcined magnesite	δ-MgO	4.6			12.4	
	β-MnO_2	7.3				
Mn minerals	δ-MnO_2	1.5				
	γ-MnO_2	5.6	6 [21]		2.8	85 [21]

It is important to point out that the material presents a large amount of amorphous minerals and very poor crystallization, since in the diffractograms, a large background

is observed and the intensity of the peaks is low in comparison with the existing Fe concentration [2]. Table 6 lists the main minerals present in the tailings and the pH value at which the surface charge of the particles is zero. These values correspond to different bibliographic sources and different measurement methods, so they are not necessarily comparable. However, it can be seen that, in many cases, the results are similar.

The results of the batch tests indicate that the adsorption preference, based on the mass retained on the CART and ACL tailings, follows the order Zn(II) > Ni(II). The high adsorption capacity of these residues, particularly in the CART, can be attributed to its higher pH and greater content of amorphous Fe (Table 2). Additionally, the adsorption capacity in the CART may be enhanced by its slightly higher CEC compared to the ACL.

The adsorption capacity of minerals formed by Fe oxides and hydroxides (ferrihydrite, hematite, and goethite) has been extensively studied by various researchers [16,20,22]. In all cases, the highest adsorption values were observed at pH levels between 6 and 7. This indicates that pH is the primary factor controlling the adsorption process in these materials, given the absence of clay minerals and the secondary role of ion exchange and chemisorption processes.

The adsorption results for Ni are consistent with studies on mineral phases of iron oxides and hydroxides similar to those in the residues under study [16,23]. These studies indicate that the highest adsorption values occur in porous media with a pH above 5. Specifically, in porous media with a pH between 6 and 7, the mobility of Ni(II) and Zn(II) is very low. Additionally, research by [24] on natural soils concludes that nickel adsorption depends on the pH and the electrolyte solution used in the experiment.

Cost–Benefit Analysis or Feasibility Study for LPRGB Applications

The environmental benefits of this approach are evident, as it proposes a practical application for tailings that are currently unused in most parts of the world. When exposed to atmospheric conditions, these tailings pose a risk of environmental contamination through wind and water erosion, due to their fine particle size and low compaction. Additionally, tailings dams have a significant visual impact on the landscape and occupy land that cannot be repurposed. Utilizing these materials in engineering applications not only mitigates these environmental and spatial issues but also reduces the demand for natural materials such as clays, loams, or silty soils, as well as synthetic alternatives like geomembranes, which are associated with higher economic costs.

From an economic standpoint, the use of these tailings is highly advantageous, as the material requires only minimal processing—primarily shredding—and is typically located near areas where industrial and urban waste landfills are planned. This proximity significantly reduces transportation and material costs, further enhancing the feasibility of their use as an alternative to conventional barrier materials

Currently, landfill sealing systems often rely on industrial materials such as PVC sheets, geotextiles, or bentonite mats. While effective, these materials have a limited lifespan, are costly, and require specialized installation. In contrast, the use of tailings presents a more economical and sustainable alternative. These materials only need to be transported and compacted at the base of the landfill, with an estimated cost of approximately 1.36 €/m^3. By comparison, the cost of impermeable clay can reach up to 80 €/m^3. This substantial cost difference, combined with the local availability of tailings and their favorable geotechnical and geochemical properties, makes them a highly attractive option for landfill barrier construction.

The applicable regulatory framework is defined by Directive (EU) 2018/850 [2], which amends Directive 1999/31/EC on the landfill of waste. This directive establishes specific requirements for the thickness and saturated hydraulic permeability of impermeable layers

used in landfill sealing systems. According to the data presented, the tailings evaluated in this study comply with these regulatory standards, confirming their suitability for use in landfill barrier applications.

Table 7 presents a comparison of the partition coefficient (K_d) value of Ni and Zn in the studied mining wastes and different natural soils. It can be observed that the value of K_d is three orders of magnitude higher than that of many of the soils mentioned in this table.

Table 7. Comparison of the partition coefficient (K_d) value of Ni and Zn in the studied mining wastes and different natural soils. In all cases, the adsorption isotherm has been fitted to the Freundlich model to obtain the values of n and K_d.

Reference	Place	Soil/Tailings			Ni(II)		Zn(II)	
			pH	CEC	n	K_d	n	K_d
[23]	Canada	Hayhook	7.5	6.3	0.373	161.9		
[24]	Denmark	Ronhave	7.0	10.9	0.775	95.4		
[20]	Louisiana	Alligator	4.8	30.2	0.939	37.8	1.011	28.1
[20]	New Mexico	Calciorthid	8.5	14.7	0.504	206.0	0.51	420
[20]	S. Carolina	Cecil	5.7	2.0	0.688	6.8	0.724	11.2
[20]	Hawaii	Kula	5.9	22.5	0.738	110.0	0.724	238
[20]	Louisiana	Lafitte	3.9	26.9	0.903	50.1	0.891	20.1
[20]	Hawaii	Molakai	6.0	11.0	0.720	44.9	0.675	80.4
[20]	Louisiana	Norwood	6.9	4.1	0.661	20.9	0.515	42.1
[20]	Louisiana	Olivier	6.6	8.6	0.646	50.5	0.625	89.1
[20]	Florida	Unnamed	4.3	2.7	0.836	3.4		
[20]	Lowa	Webster	7.6	48.1	0.748	3.4	0.697	774
[20]	N. Hampshire	Windsor	5.3	2.0	0.741	8.4	0.792	9.68
this study	Moa, Cuba	ACL	6.5	10.0	0.101	1351	0.11	1962
this study	Cartagena, Spain	CART	7.88	18.7	0.24	1194	0.15	2347

6. Conclusions

Laboratory tests indicate that CART and ACL mining-metallurgical tailings exhibit a higher adsorption capacity than several natural soils (Table 4), with a very high partition coefficient (K_d). Given the metal adsorption properties of these wastes, they can be considered a viable alternative for constructing LPRGB. This is further supported by their low permeability, which is 10^{-8} m/s under natural conditions and decreases when compacted [3,25,26]. Considering that regulations for constructing impermeable barriers in mining, metallurgical, hazardous industrial, and urban waste deposits require a maximum permeability of 10^{-9} m/s, these wastes are suitable for this purpose. This conclusion is based on flow and transport tests of heavy metals under permeability conditions consistent with current legislation.

It is evident that using a metal concentration of 416 mg/L requires renewing the volume of water stored in the porous medium at least 23 times. During the desertification process, the residues retain most of the soil mass, demonstrating their ability to fix metals in the medium. Additionally, the release of metals is slow and occurs at low concentrations. This indicates the potential of these wastes to be used as LPRGB, as it is possible to determine the volume of waste leachate that will saturate the material if the effluent characteristics are known.

The leachate characteristics of waste can be studied in the laboratory. Based on the metal concentration in the leachate, it is possible to determine the volume of these materials that should be placed at the bottom of the tank to ensure environmentally safe waste storage.

Moreover, the reuse of mining tailings in landfill barrier systems offers a compelling solution that aligns environmental sustainability with economic efficiency. By transforming a problematic waste product into a valuable construction material, this approach not only addresses pressing ecological concerns—such as land degradation, contamination risks, and resource depletion—but also presents a cost-effective alternative to conventional materials. The compliance of these tailings with EU regulatory standards further reinforces their viability, paving the way for broader adoption in waste management infrastructure. As such, this strategy represents a forward-thinking step toward more sustainable and circular practices in both the mining and waste disposal sectors.

Author Contributions: Conceptualization, R.R.-P.; methodology, R.R.-P.; writing—original draft preparation, R.R.-P. and J.B.; writing—review and editing, J.B. and A.O.O.-G. All authors have read and agreed to the published version of the manuscript.

Funding: The authors thank to Ministry for Ecological Transition and Demographic Challenges (MITECO), Dirección General de Biodiversidad for funding this research: TD by PRTR Medida C04.I03 belonging to "Asesoramiento en actuaciones de restauración de zonas mineras en el entorno del Mar Menor" Project (J. Butlanska) and "Estudio de las materias primas críticas y estratégicas para la transición ecológica y el suministro de las principales cadenas de valor industrial en España" Project—MPMIN ref. 3263 (A. O. Oliva-González). This work was also supported by grant PID2022-138197OB-100 funded by MICIU/AEI/10.13039/50100011033 and by ERDF/E (R. Rodríguez-Pacheco)".

Data Availability Statement: The original contributions presented in this study are included in the article. Further inquiries can be directed to the corresponding authors.

Acknowledgments: The anonymous reviewers are thanked for their contribution, which has substantially improved and enriched the work.

Conflicts of Interest: The authors declare no conflicts of interest. The funders had no role in the design of the study, in the collection, analyses, or interpretation of data, in the writing of the manuscript, or in the decision to publish the results.

References

1. Obiri-Nyarko, F.; Grajales-Mesa, S.J.; Malina, G. An overview of permeable reactive barriers for in situ sustainable groundwater remediation. *Chemosphere* **2014**, *111*, 243–259. [CrossRef] [PubMed]
2. Directive (EU) 2018/850 of the European Parliament and of the Council of 30 May 2018 amending Directive 1999/31/EC on the landfill of waste. Available online: https://eur-lex.europa.eu/legal-content/EN/TXT/?uri=celex:32018L0850 (accessed on 15 January 2025).
3. Rodríguez, R. Estudio Experimental de Flujo y Transporte de Cromo, Níquel y Manganeso en Residuos de la Zona Minera de Moa (Cuba): Influencia del Comportamiento Hidromecánico. Ph.D. Thesis, Universidad Politécnica de Catalunya (UPC), Barcelona, Spain, 2002.
4. Rodríguez-Pacheco, R.; Candela, L.; Hidalgo, M.; Salvado, V.; Queralt, I.; Lloret, A. Evaluación de la capacidad de adsorción de dos residuos mineros para su posible uso en barreras geoquímicas reactivas de baja permeabilidad. In Proceedings of the Geo-Temas: VI Congreso Geológico de España, Zaragoza, Spain, 12–15 July 2004; ISSN 1567–5172.
5. Rodríguez, R.; Candela, L. Transport of Cr(VI), Ni(II) and Mn(II) trough metallurgical waste. Batch and column experiments. In *Reactive Transport in Soil and Groundwater*; Nutzmann, G., Viotti, P., Aagaard, P., Eds.; Springer: Dordrecht, The Netherlands, 2005; pp. 65–77.
6. Blowes, D.W.; Ptacek, C.J.; Jambor, J.L. In situ remediation of Cr(VI)-contamiannted ground water. Using permeable reactive walls. *Env. Sci. Tech.* **1997**, *31*, 3348–3357. [CrossRef]
7. USEPA 2021. A Community Guide to Permeable Reactive Barriers. Office of Land and Emergency Management (5203P) | EPA-542-F-21-019. 2021. Available online: www.clu-in.org (accessed on 14 January 2025).
8. FRTR 2025. Federal Remediation Technologies Roundtable. Available online: https://www.frtr.gov/matrix-2019/Permeable-Reactive-Barriers/ (accessed on 14 January 2025).

9. *DIN 38414-S4*; German Standard Methods for the Examination of Water, Waste Water and Sludge; Sludge and Sediments (Group S); Determination of Leachability by Water (S 4). Determination of Leachability by Water. Institutfür Normung: Berlin, Germany, 1984.
10. Robles-Arenas, V.M.; Rodríguez, R.; García, C.; Manteca, J.I.; Candela, L. Sulphide-mining impacts in the physical environment: Sierra de Cartagena-La Unión (SE Spain) case study. *Environ. Geol.* **2006**, *51*, 57–64. [CrossRef]
11. Alcolea, A. Geoavailability of Ni, Cu, Zn, As, Cd, and Pb in th, e Sierra de Cartagena-La Unión (SE Spain). Doctoral Thesis, Universidad Politécnica de Cartagena, Departamento de Ingeniería Minera, Geológica y Cartográfica, Cartagena, Murcia, Spain, 2015.
12. Rodríguez-Pacheco, R.; García, G.; Caparrós-Ríos, A.V.; Robles-Arenas, V.; García-García, C.; Millán, R.; Pérez-Sanz, A.; Alcolea-Rubio, L.A. Mineralogy, Geochemistry and Environmental Hazards of Different Types of Mining Waste from a Former Mediterranean Metal Mining Area. *Land* **2023**, *12*, 499. [CrossRef]
13. Selim, H.M.; Amacher, C. *Reactivity and Transport of Heavy Metals in Soils*; Lewis Publishers: New York, NY, USA, 1997.
14. Aris, R. On the dispersion of linear kinematic waves. *Proc. R. Soc. Lond. Ser. A.* **1958**, *245*, 268–277.
15. BOE, 30 de abril de 1986. Criterios relativos a los límites de vertidos. Available online: https://www.boe.es/eli/es/rd/1986/04/11/849/con (accessed on 30 January 2025).
16. Sparks, D.L. Ion exchange processes. In *Chapter 6: Environmental Soil Chemistry*; Academic Press: New York, NY, USA, 1995; pp. 141–158.
17. Appelo, C.A.J.; Postma, D. *Geochemistry Groundwater and Pollution*; A.A. Balkema: Rotterdam, The Netherlands, 1993.
18. Anderson, M.A.; Rubin, A.J. Adsorption of inorganics at soil-liquid interfaces. *Soil Sci.* **1982**, *133*, 257–258. [CrossRef]
19. Tan, K.H. Electrochemical properties of solid constituents. In *Chapter 6. Environmental Soil Science*; Dekker, M., Ed.; INC.: New York, NY, USA, 1994.
20. McKenzie, R.M. The adsorption of lead and other heavy metals on oxides of manganese and iron. *Aust. J. Soil Res.* **1980**, *18*, 61–73. [CrossRef]
21. Stollenwerk, K.G. Geochemical interactions between constituents in acidic groundwater and alluvium in an aquifer near Globe, Arizona. *Appl. Geochem.* **1994**, *9*, 353–369. [CrossRef]
22. Payne, T.E.; Lumpkin, G.R.; Waite, T.D. UraniumVI adsorption on model minerals: Controlling factors and surface complexation modeling. In *Adsorption of Metals by Geomedia*; Jenne, E.A., Ed.; Academic Press: New York, NY, USA, 1998; Volume 583, pp. 75–97. [CrossRef]
23. Wang, W.Z.; Brusseau, M.L.; Artiola, J. Nonequilibrium and Nonlinear Sorption during Transport of Cadmium, Nickel, and Strontium through Subsurface Soils. In *Adsorption of Metals by Geomedia*; Jenne, E.A., Ed.; Academic Press: New York, NY, USA, 1998; Volume 583, pp. 427–443. [CrossRef]
24. Poulsen, I.F.; Bruun, H.C. Soil sorption of nickel in presence of citrate or arginine. *Water Air Pollut.* **2000**, *120*, 249–259. [CrossRef]
25. Buchter, B.; Davidoff, B.; Amacher, M.C.; Hinz, C.; Iskandar, I.K.; Selim, H.M. Correlation of Freundlich Kd and n retention parameters with soils and elements. *Soil Sci.* **1989**, *148*, 370–379. [CrossRef]
26. Smith, K.S.; Ranville, J.F.; Plumlee, G.S.; Macalady, D.L. Predictive double layer modeling of metal sorption in mine drainage systems. In *Chapter 24: Adsorption of metals by Geomedia*; Academic Press: New York, NY, USA, 1998. [CrossRef]

Disclaimer/Publisher's Note: The statements, opinions and data contained in all publications are solely those of the individual author(s) and contributor(s) and not of MDPI and/or the editor(s). MDPI and/or the editor(s) disclaim responsibility for any injury to people or property resulting from any ideas, methods, instructions or products referred to in the content.